Proceedings of the 3rd Croatian Conference on Earthquake Engineering - 3CroCEE
19–22 March 2025, Split, Croatia

DOI: https://doi.org/10.5592/CO/3CroCEE.2025.86

NEAR-DISTANCE SPECTRAL PARAMETER KAPPA CALCULATIONS FOR STATIONS INSTALLED IN N. MACEDONIA

Marina Poposka [(1)], Davor Stanko [(2)], Radmila Salic Makreska [(3)], Dragi Dojcinovski [(4)] Marta Stojmanovska [(5)]

[(1)] *Research Assistant, Ss. Cyril and Methodius University in Skopje, Institute of Earthquake Engineering and Engineering Seismology, Skopje, R. N. Macedonia, marina@iziis.ukim.edu.mk*
[(2)] *Assistant Professor, Faculty of Geotechnical Engineering, University of Zagreb, Varaždin, Croatia, dstanko@gfv.hr*
[(3)] *Full Professor, Ss. Cyril and Methodius University in Skopje, Institute of Earthquake Engineering and Engineering Seismology, Skopje, R. N. Macedonia, r_salic@iziis.ukim.edu.mk*
[(4)] *Full Professor, Ss. Cyril and Methodius University in Skopje, Institute of Earthquake Engineering and Engineering Seismology, Skopje, R. N. Macedonia, dragidoj1@yahoo.com*
[(5)] *Associate Professor, Ss. Cyril and Methodius University in Skopje, Institute of Earthquake Engineering and Engineering Seismology, Skopje, R. N. Macedonia, marta@iziis.ukim.edu.mk*

Abstract

The objective of this study is to estimate the high-frequency decay parameter – kappa (κ) for stations installed in the regions with highest seismicity in North Macedonia.

Kappa characterizes the attenuation of ground motion at high frequencies, more precisely defines the rate of decrease of the acceleration amplitude spectrum. At higher frequencies ground motions on rock may be larger than those on soil due to lesser damping from impedance contrasts in the near-surface. Thus, site effects on rock are an important topic for structures that are sensitive to high frequencies.

Comparison of kappa estimated values is made using strong motion data obtained from four different locations Pehcevo (PEH), Ohrid (OHR), Debar (DBR), and Valandovo (VAL). Local site condition parameters, specifically V_{S30}, are determined for each station based on conducted geophysical investigations and/or microtremor measurements. The accelerometric data used for analysis are obtained from local earthquake events within a magnitude range (M_w) of 3.0 to 5.5, epicentral distances (R_{epi}) less than 120 km, and focal depths (h) less than 40 km. The data were visually inspected, baseline corrected, and a bandpass filter was applied. Earthquake records with SNR<3 were excluded from the analysis.

The value of kappa is estimated from the acceleration amplitude spectrum of shear waves from the slope of the high-frequency part where the spectrum starts to decay rapidly to a noise level.

Based on the results obtained, conclusions are drawn regarding the impact of this parameter on the attenuation of near-surface crust rock layers, as well as local effects in near-distances.

Keywords: kappa, FAS, near-surface attenuation, strong motion data

1. Introduction

The Republic of North Macedonia is a seismically active region with low to moderate seismicity, though some areas exhibit nearly high levels of seismic activity. In the past, numerous earthquakes struck the country's territory, with some devastating almost entire cities. For instance, in the past century, the most significant earthquakes that occur in the N. Macedonia are Pehchevo earthquake 1904 (M=7.5, I=10), Valandovo earthquake 1931 (M=6.7, I=10), Skopje earthquake 1963 (M=6.1, I=9), Debar earthquake 1967 (M=6.5, I=9). Based on the effects of these events, these regions in North Macedonia are where the expected seismic hazard level is the highest.

Over the years, various studies have been conducted to assess the seismic hazard in this country. However, no study has yet focused on the local attenuation of seismic waves at high frequencies. To

DOI: https://doi.org/10.5592/CO/3CroCEE.2025.86

characterize these effects, Anderson and Hough (1984) introduced the empirical high-frequency decay parameter *kappa* (κ), aiming to explain deviations in the shape of the spectral acceleration curve from the theoretical Brune's model (1970) at frequencies higher than the source corner frequency. Using earthquake records with magnitudes greater than 5, they calculated the spectral parameter kappa for different stations by analyzing log-linear spectral space within constrained frequency ranges. Currently are available many approaches for estimating kappa (Ktenidou et. al 2014), and this parameter is widely used for site characterization, especially given empirical k_0-V_{S30} correlations (Silva et al. 1999, Chandler et al.2005, Drouet et al. 2010, Edwards et al. 2011, Van Heute et al. 2011, Ktenidou et al., 2013, 2014, 2015, Stanko et al. 2017), among other uses such site amplification (Boore et al. 1997), input parameters for creation and calibration of GMPEs, host to target adjustments of GMPEs to different regions (Cotton et al. 2006; Douglas et al. 2006; Biro and Renault 2012), as well as its correlation with engineering parameters like peak ground acceleration (PGA) and Arias intensity (Mena et al. 2010).

Despite its importance, there are no prior studies in North Macedonia focusing on the high-frequency decay parameter to quantify the effect of near-surface geology on seismic waves.

The IZIIS strong motion network with accelerometers installed across N. Macedonia at various locations and on different types of soil types provide valuable data for further research and estimation of the high-frequency decay parameter. In this study, records from earthquakes with magnitudes (M_w) higher than 3 and epicentral distances (R_{epi}) of less than 120 km were analyzed, collected from four locations in North Macedonia

The study begins with an overview of the study area and the description of strong motion records, followed by an evaluation of the method used for kappa calculation. The results are then presented and discussed, with appropriate conclusions drawn.

2. Study area and strong motion records

For this study, the regions with the highest seismicity in North Macedonia were analyzed (Fig. 1). Using information from historical and recent seismic events, along with EC8 seismic hazard zoning maps (Milutinovic at al.2016), four stations—PEH, OHR, DBR, and VAL from the IZIIS strong motion network were selected. These stations, located in the regions where the hazard level is the highest, provided strong motion records obtained from 200 Hz sampling accelerometers (Guralp CMG-5TD and ETNA-2). Site characteristics were determined through geophysical measurements (Seismic Refraction Tomography - SRT or/and Multichannel Analysis of Surface Waves - MASW) for the OHR, PEH and DBR stations (Stojmanovska et al. 2020-2021, Garevski et.al. 2016), while HVSR (horizontal to vertical spectral ratio) from earthquake records using the Konno and Ohmachi [1998] (b-value=20) smoothed Fourier amplitude spectrum was conducted for all four stations to obtain the predominant site frequency and possible site amplifications.

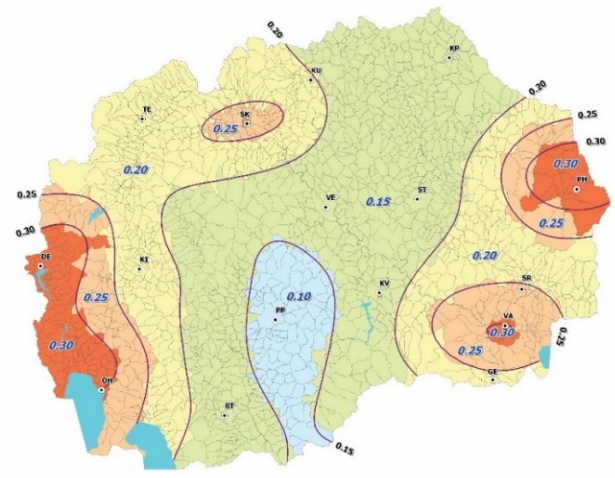

Figure 1. Seismic hazard zoning maps return period T=475 years (Milutinovic at al.2016)

DOI: https://doi.org/10.5592/CO/3CroCEE.2025.86

Between 2011 and 2024, these stations recorded 221 earthquake events with magnitudes ranging from 2.11 to 6.4 and epicentral distances from 1.66 to 430 km. To exclude the possibility of source effects on kappa calculation, only records with magnitudes greater than 3, while for the epicentral distances up to 120 km were considered for this analysis. Fig. 2 presents the spatial distribution of the earthquakes recorded in these stations, and station locations with blue triangles.

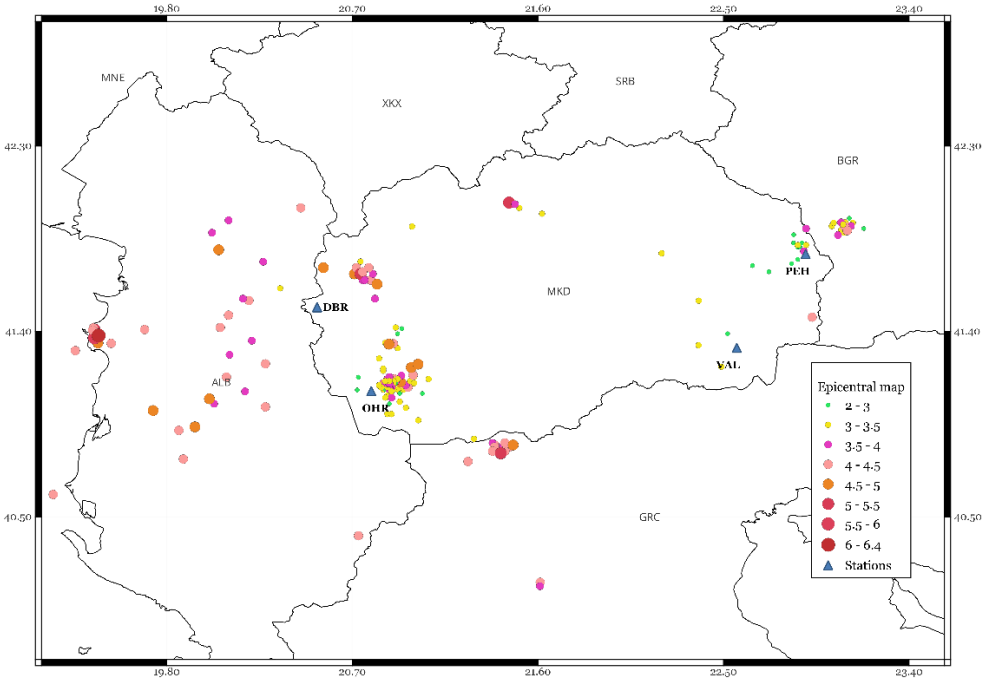

Figure 2. Spatial distribution of earthquake and station locations in the research area.

Table 1 provides station location information, soil type, investigation type, and number of earthquake records included in the analysis. The data included in the analysis are constrained based on the recommendations for higher-quality analysis provided in the following text. Fig. 3 shows the horizontal to vertical spectral ratios (HVSR) derived from earthquakes for the four stations.

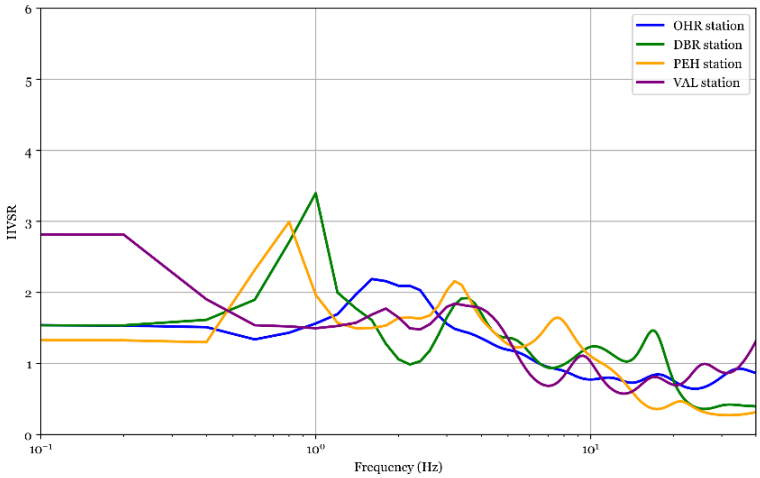

Figure 3. Horizontal to Vertical Spectral Ratios (HVSR) from earthquake records using the Konno and Ohmachi [1998] (b-value=20) smoothed Fourier amplitude spectrum for four stations.

According to Fig. 3 the observed predominant site frequencies fall within the frequency range of 0.6 to 5 Hz. To exclude potential effects on the estimation of kappa (Parolai and Bindi (2004)), the minimum value for boundary frequency f_{1min} is set to 10 Hz.

Proceedings of the 3rd Croatian Conference on Earthquake Engineering - 3CroCEE
19–22 March 2025, Split, Croatia

DOI: https://doi.org/10.5592/CO/3CroCEE.2025.86

Table 1. Station information, investigation type 1- geophysics, type 2 – HVSR, number of earthquake data recorded per station

Station	Latitude [°]	Longitude [°]	V_{s30} [m/s]	Investigation type	Number of earthquake records
OHR	41.111389	20.792222	1000	1, 2	68
DBR	41.518556	20.529361	400-450	1, 2	148
PEH	41.776278	22.897861	380-450	1, 2	50
VAL	41.321528	22.564528	600-800	2	38

3. Signal processing and kappa calculation

The records obtained from the seismic sensors were organized according to the magnitude, epicentral distance, and depth of the earthquake (Fig. 4, green dots representing analyzed data, while blue, yellow, grey, and red dots representing neglected data where M_w<3, R_{epi}>120, and SNR<3). The data were visually inspected, baseline corrected, and a bandpass filter ranging from 0.1 to 100 Hz was applied. Bad quality data, data with SNR < 3, and data with S-window portion less than 4 seconds (to ensure good spectral resolution) were excluded from the analysis.

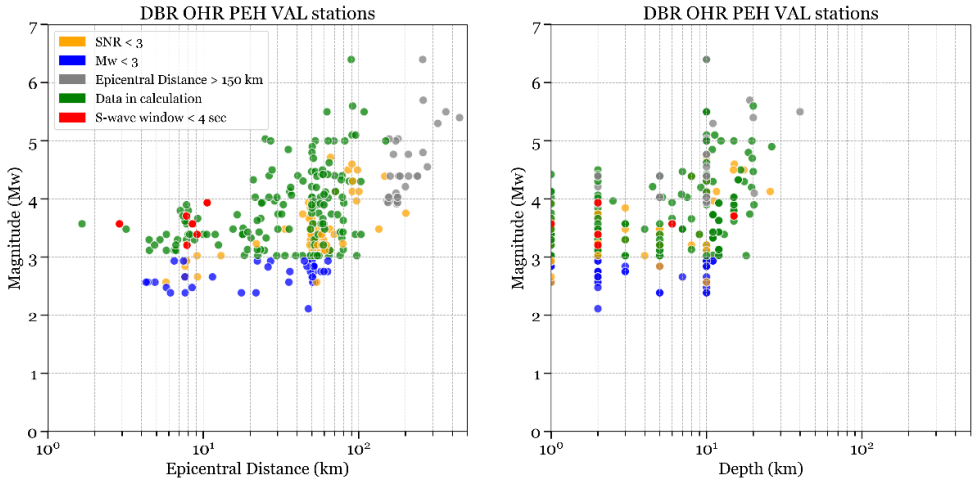

Figure 4. Statistics of the compiled ground motion dataset. (a) R_{epi}-M_W distribution of recordings (b) h-M_W distribution of recordings

As a method for kappa calculation, the original acceleration spectral method (Anderson & Hough, 1984), using the S-wave window and recommended procedure in Ktenidou et al. 2014, was employed. S-wave windows (longer than 4 seconds) and noise windows were manually selected (Fig. 5, first row). A 5% cosine taper was applied to both windows, followed by the calculation of the Fourier Amplitude Spectrum (FAS) (Fig. 5, middle row). Using the earthquake parameters, the corner frequency f_c and the theoretical spectrum, based on Brune's model, were calculated (Fig. 5 – black line). The frequencies f_1 and f_2 were manually selected: f_1 was chosen to be greater than $1.5f_c$ to ensure the source contribution would not bias the kappa calculation, and if f_1<10 Hz, f_1=10 Hz to avoid the influence of possible site resonance. f_2 was selected where the spectrum becomes flat and to ensure that the signal-to-noise ratio (SNR) between the S-wave and noise windows was greater than 3. Kappa was determined from the slope of the FAS in the linear-logarithmic space within the frequency range between f_1 and f_2 (Fig. 5 – blue line). The frequency band Δf was with min value of 10. Spectra with ranges of Δf < 10 Hz were discarded in the interest of the robustness of the slope computation. Depending on the magnitude and distance of the event, the frequency f_1 ranges from 10 to 17 Hz and, while f_2 is between 25 and 40 Hz. The Nyquist frequency based on sampling rate is 100 Hz and the instrument response does not exhibit decay below 60 Hz, so a rather large range of frequencies can be used for κappa computations.

Proceedings of the 3rd Croatian Conference on Earthquake Engineering - 3CroCEE
19–22 March 2025, Split, Croatia

DOI: https://doi.org/10.5592/CO/3CroCEE.2025.86

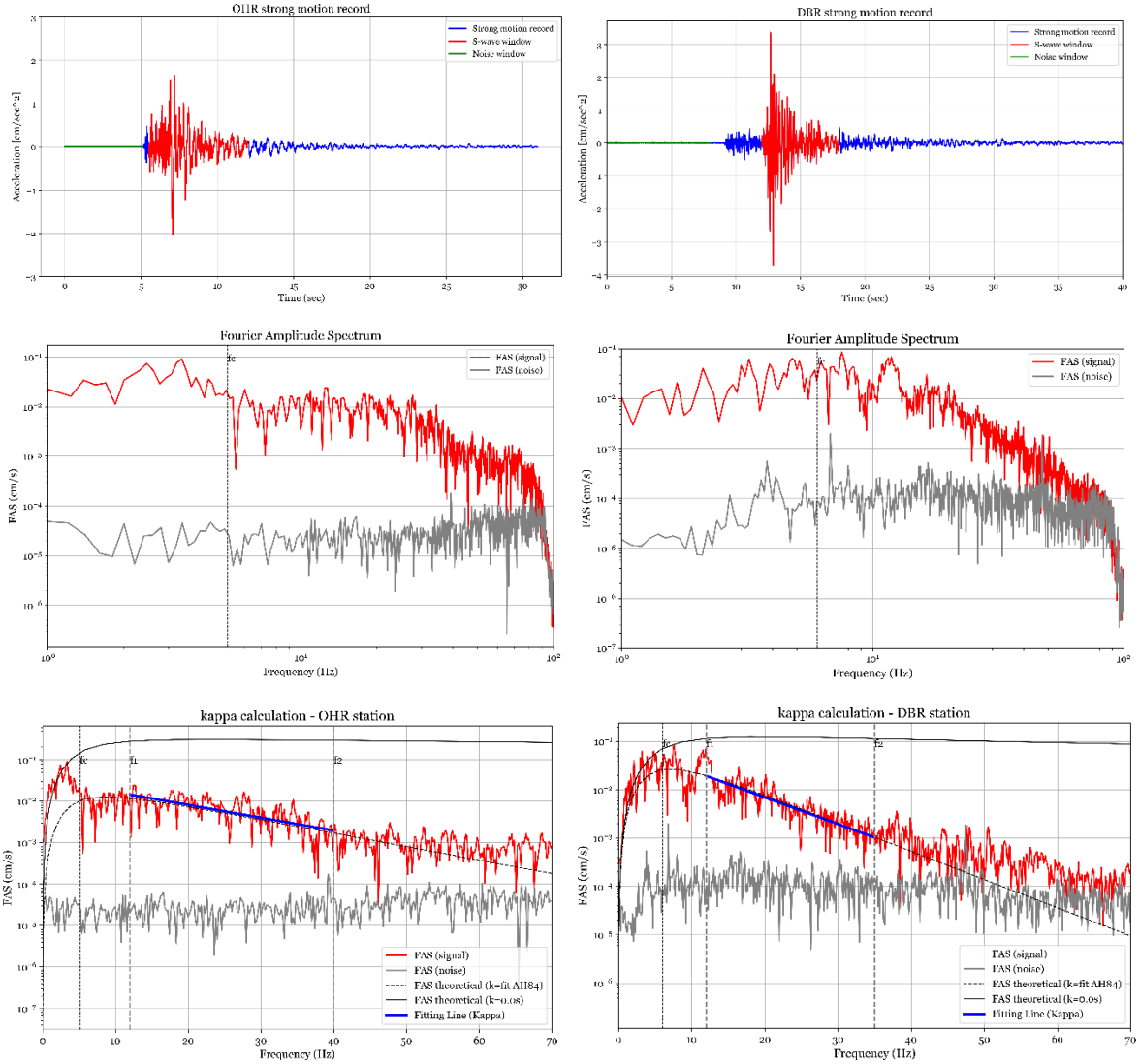

Figure 5. Example of kappa calculation for OHR station - NS component for earthquake event with Mw =3.8, Re = 8.01 km, k = 0.0226s and DBR station – NS component for earthquake event with Mw =3.66, Re = 23.5 km, k= 0.0407s

Fig. 5 presents the procedure for kappa calculation. Two stations are shown: OHR, located on rock (type A according to EC8), and DBR, located on soil type B. The records are horizontal components from earthquakes with magnitude M_w=3.8 and R_{epi}=8.01km for the OHR station, and M_w=3.66 and R_{epi}=23.5 km for the DBR station. The obtained kappa values for these records are k=0.0226s for OHR and k=0.0407s for DBR station. The slope of the FAS is expected to be less steep for OHR (soil type A) and steeper for DBR (soil type B).

4. Results

Using York regression analysis (York et al. 2014) with errors in both variables, kappa for one standard deviation and R_{epi} for 3 km, the high-frequency decay parameter was calculated for four stations. Two of the stations are presented in Fig. 6, while the results for all four stations are provided in Table 2. The site component (k_0) was obtained from the regression line extrapolated to 0 distance, as well as from the mean value of the records up to 25 km for the stations where the majority of the data were from near

DOI: https://doi.org/10.5592/CO/3CroCEE.2025.86

distances. Averaged values for the two horizontal components with a difference of less than 25% were considered, while the others were excluded from the regression. Exceptions were made for stations with a small number of records at close distances, allowing high-quality data with differences larger than 25% to be taken into account.

The regression analysis was performed twice: once using the full dataset (Fig. 6, blue line) and once excluding the outliers in one standard deviation (Fig. 5, red dashed line). There is not a significant difference between the results obtained, except for the coefficient of determination (R^2) for both regressions. The York regression without outliers provides kappa calculation with higher R^2 values, indicating a better fit of the data.

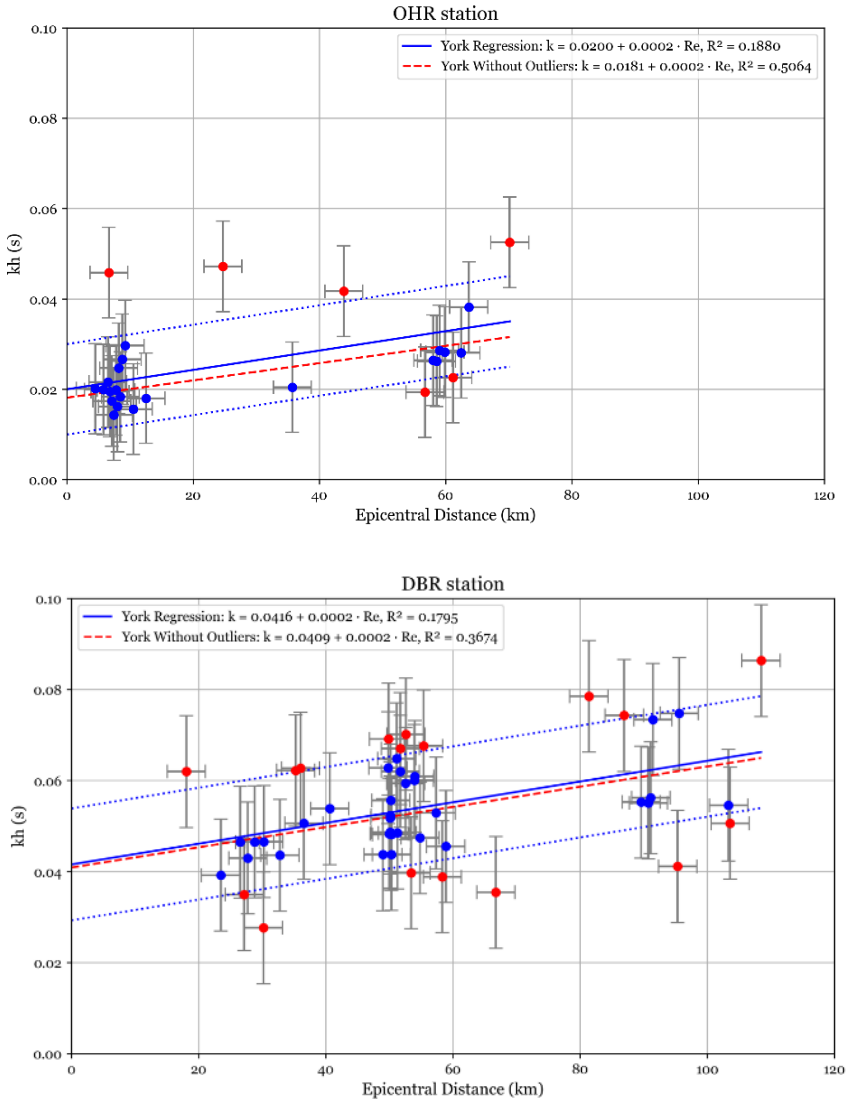

Figure 6. Distribution of individual κappa values and regression with distance for stations (OHR station up) and (DBR station down). Regressed lines plotted ± 1 standard deviation.Vertical error-bars show the uncertainty of κappa values and horizontal error-bars show uncertainty in epicentral distances with standard error set to ± 3 km.

In Fig. 6, the difference in local attenuation due to soil effects is clearly observable. For the station embedded in rock, lower values of local attenuation are observed, whereas higher values are evident for the station located on looser soil. Table 2 presents the site-specific parameter values obtained for the four stations using regression analysis and mean values up to 25 km for each station. If the number of records at close distances was at least 10, the mean value was chosen.

DOI: https://doi.org/10.5592/CO/3CroCEE.2025.86

Table 2. Site component (k_0) values obtained from regression analysis using error-in-variables and mean values for distances up to 25 km, along with the number of records included in each analysis and V_{S30} values for each station

Station	k_0 regression	No. records	k_0 mean up to 25 km	No. records (0-25km)	$V_{s,30}$ [m/s]
OHR	0.0181±0.003	28	0.0232	16	1000
DBR	0.0408±0.006	49	0.0506	2	400-450
PEH	0.0281±0.010	10	0.0396	10	380-450
VAL	0.0317±0.008	9	0.0320	2	600-800

The V_{S30} values for the stations range from 380 to 1000 m/s, corresponding to two soil types, A and B, according to the EC8 classification. Fig. 7 (an updated version based on Ktenidou et al. (2014) and Stanko et al. (2017)) presents the compiled κ_0–V_{S30} values for various global regions where κ_0 was calculated using the AH84 method, alongside the measured κ_0 and V_{S30} values for stations in North Macedonia. This figure demonstrates that the near-site attenuation (κ_0) values observed for North Macedonian stations are closely aligned with the global κ_0 values reported in previous studies.

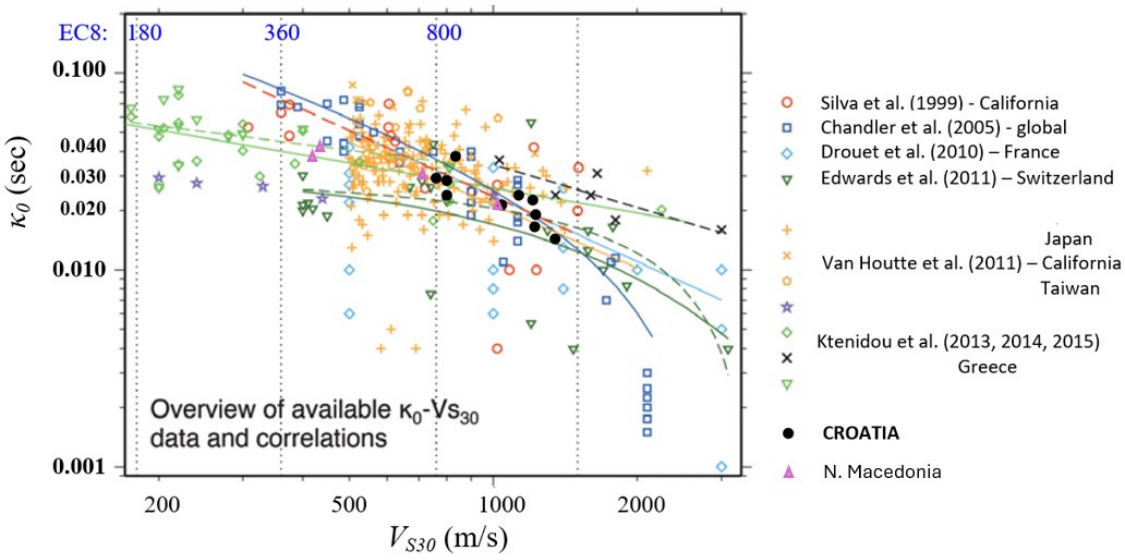

Figure 7. Existing κ_0–V_{S30} correlations in the literature (coloured markers and their fit lines for particular regions are shown in legend). Adapted from Ktenidou et al. (2014) and Stanko et al. (2017). κ_0 and $V_{S,30}$ values for N. Macedonian stations are shown by pink triangles. Site $V_{S,30}$ classes according to EC 8 (blue numbers) are shown above plot.

Fig. 8 shows a 3D plot of kappa values as a function of earthquake magnitude and epicentral distance for station installed on rock (OHR station, Fig.8 left) and for stations on soil (DBR, PEH, VAL stations, Fig.8 right). Lower values for the high - frequency parameter is obtained for OHR – rock station. Fig. 9 presents two 2D plots showing the same correlations for all the stations combined. It is noticeable that the values increase with distance, while there is no particular correlation with magnitude especially for range in 3 to 4. Earthquakes with high magnitudes and close distances are sparse, so it can't be evaluated the magnitude impact on kappa for higher magnitude values in close distance.

DOI: https://doi.org/10.5592/CO/3CroCEE.2025.86

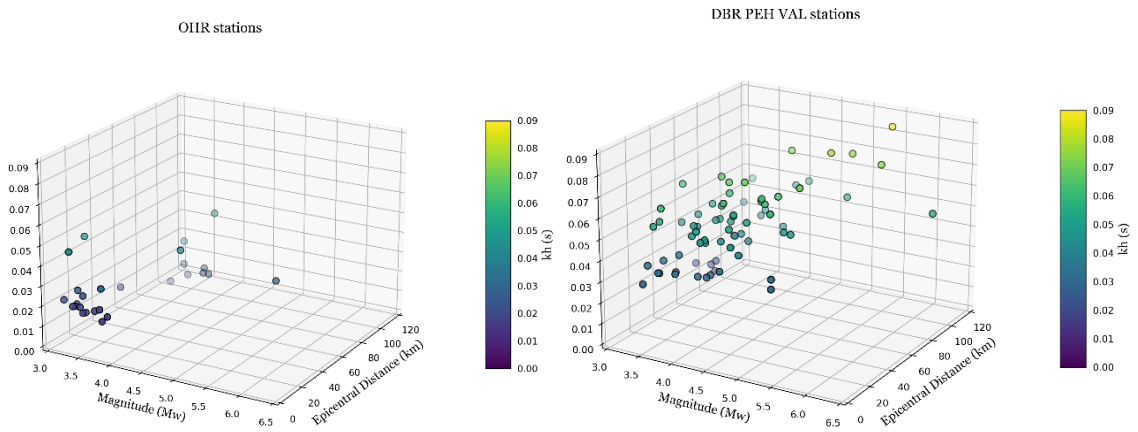

Figure 8. 3D plot of obtained results for kappa in correlation with M_w and R_{epi}

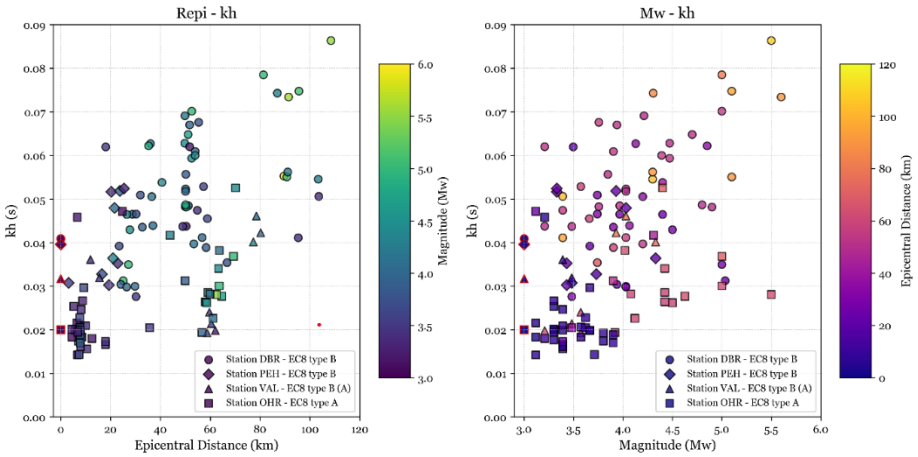

Figure 9. Correlation of kappa parameter with epicentral distance (R_{epi}) and Moment magnitude (M_w), site-specific component k_0 for each station is marked as a symbol with red outline

5. Conclusion

In this article, the kappa parameter and its site–specific component was estimated for four station locations in North Macedonia. For the calculation good – quality earthquake records from the IZIIS strong motion network were used. It was investigated the parameter dependance on epicentral distance, site conditions, and earthquake magnitude. The results from this study could be valuable related to attenuation ground modelling and updating seismic hazard maps in the region.

The observed results provide an estimated correlation with the magnitude and distance of the occurred earthquakes in the region.

It can be seen a suitable correlation with the soil conditions on the analyzed locations. Owing to geological conditions, sites with higher shear wave velocity exhibit lower k_o values, while for lower share wave velocity exhibit higher values corresponding to a region with significant attenuation. The estimated values for the OHR station (V_{s30}=1000m/s) are k_0=0.0232s, while for the VAL (V_{s30} = 600-800m/s), DBR (V_{s30}=400-450m/s), and PEH (V_{s30}=380-450m/s) are k_0=0.0317s, k_0=0.0408s, and k_0=0.0396s, respectively. The obtained results are consistent with the expected range observed in previous studies conducted in other countries.

DOI: https://doi.org/10.5592/CO/3CroCEE.2025.86

References:

[1] Anderson, J., Hough, S. (1984): A model for the shape of the Fourier amplitude spectrum of acceleration at high frequencies. Bulletin of the Seismological Society of America, 74(5), 1969–1993. doi: 10.1785/BSSA0740051969.

[2] Boore, D.M., Joyner, W. (1997): Site amplifications for generic rock sites. Bulletin of the Seismological Society of America, 87(2), 327–341.

[3] Biro, Y., Renault, P. (2012): Importance and impact of host-to-target conversions for ground motion prediction equations in PSHA. Proceedings of the 15th World Conference of Earthquake Engineering, Lisbon, Portugal.

[4] Brune, J.N. (1970): Tectonic stress and the spectra of seismic shear waves from earthquakes. Journal of Geophysical Research, 75, 4997–5009. doi: 10.1029/JB075i026p04997.

[5] Cotton, F., Scherbaum, F., Bommer, J.J., Bungum, H. (2006): Criteria for selecting and adjusting ground-motion models for specific target regions: Application to Central Europe and rock sites. Journal of Seismology, 10, 137–156.

[6] Douglas, J., Bungum, H., Scherbaum, F. (2006): Ground motion prediction equations for southern Spain and southern Norway obtained using the composite model perspective. Journal of Earthquake Engineering, 10, 33–72.

[7] Douglas J, Gehl P, Bonilla LF, Gelis C. (2010): A j model for mainland France. Pure Appl Geophys. 167(11):1303–1315. doi: 10.1007/s00024-010-0146-5.

[8] Edwards, B., Fäh, D., Giardini, D. (2011): Attenuation of seismic shear wave energy in Switzerland. Geophysical Journal International, 185, 967–984. doi: 10.1111/j.1365-246X.2011.04987.

[9] Garevski, M., Gjorgjevska, I., Dojchinovski, D. (2016): Geophysical investigations - Pedestrian bridge in Ohrid (Center-Kaneo), Pangea Inzenering Report No. 08-39, 2016.

[10] Konno K. and T. Ohmachi (1998): Ground motion characteristics estimated from spectral ratio between horizontal and vertical components of microtremor, Bull. Seism. Soc. Am. 88, 228–241.

[11] Ktenidou, O.J., Gelis, C., Bonilla, L.F. (2013): A study on the variability of kappa (κ) in a borehole: Implications of the computation process. Bulletin of the Seismological Society of America, 103(2A), 1048–1068. doi: 10.1785/0120120093.

[12] Ktenidou, O., Cotton, F., Abrahamson, N.A., Anderson, J.G. (2014): Taxonomy of κ: A review of definitions and estimation approaches targeted to applications. Seismological Research Letters, 85, 135–146. doi: 10.1785/0220130027.

[13] Ktenidou, O.J., Abrahamson, N.A., Darragh, R.B., Silva, W.J. (2016): A methodology for the estimation of kappa (κ) from large datasets: Example application to rock sites in the NGA-East database and implications on design motions. PEER Report No. 2016/01.

[14] Milutinovic, Z., Salic, R., Dumurdzanov, N., et al. (2016): Seismic zoning maps for Republic of Macedonia according to the requirements of MKS-EN 1998-1:2004 - Eurocode 8. IZIIS Report, 2016-26.

[15] Palmer, S. M. (2022): Examining κ, the high frequency spectral decay parameter, in Eastern Canada, Electronic Thesis and Dissertation Repository. 8680. https://ir.lib.uwo.ca/etd/8680.

[16] Palmer, S. M., Atkinson G. M. (2020): High frequency decay slope of spectra (kappa) for M≥3.5 earthquakes on rock sites in eastern and western Canada, Bull. Seism. Am. 110(2), 471-488. Doi: 10.1785/0120190206.

[17] Parolai, S., Bindi, D. (2004): Influence of soil-layer properties on κ evaluation. Bulletin of the Seismological Society of America, 94, 349–356.

[18] Silva, W., Darragh, R., Gregor, N., Martin, G., Abrahamson, N., Kircher, C. (1998): Reassessment of site coefficients and near-fault factors for building code provisions. Technical Report Program Element II: 98-HQGR-1010, Pacific Engineering and Analysis, El Cerrito, USA.

[19] Stanko, D., S. Markusic, T. Korbar, and J. Ivancic (2020): Estimation of the high frequency attenuation parameter kappa for the Zagreb (Croatia) seismic stations, Applied Sciences 10, doi: 10.3390/app10248974.

DOI: https://doi.org/10.5592/CO/3CroCEE.2025.86

[20] Stojmanovska, M., Dojcinovski, D., et al. (2020–2021): Development and upgrading of strong motion network, Phase 1: Database, website, and unified approach to signal processing. Report IZIIS 2021-66, financed by the Institute of Earthquake Engineering and Engineering Seismology, UKIM, Skopje, North Macedonia.

[21] Van Houtte, C., Drouet, S., Cotton, F. (2011): Analysis of the origins of κ (kappa) to compute hard rock to rock adjustment factors for GMPEs. Bulletin of the Seismological Society of America, 101(6), 2926–2941. doi: 10.1785/0120100345.

[22] York, D., Evenson, N., Martinez, M., Delgado, J. (2004): Unified equations for the slope, intercept, and standard errors of the best straight line. American Journal of Physics, 72, 367–375.